UC Santa Barbara
UC Santa Barbara Previously Published Works

Title

The adsorption/desorption of phosphorus in freshwater sediments from buffer zones: the effects of sediment concentration and pH

Permalink

https://escholarship.org/uc/item/8ht0w6tq

Journal

Environmental Monitoring and Assessment, 188(1)

ISSN

0167-6369

Authors

Zhang, Liang
Du, Yun
Du, Chao
et al.

Publication Date

2016

DOI

10.1007/s10661-015-5018-0

Peer reviewed

The adsorption/desorption of phosphorus in freshwater sediments from buffer zones: the effects of sediment concentration and pH

Liang Zhang · Yun Du · Chao Du · Meng Xu · Hugo A. Loáiciga

Abstract Riparian buffer zones adjacent to reservoirs and lakes protect aquatic ecosystems from polluted surface runoff. Sediments, collected from the buffer zones of Danjiangkou Reservoir (S_R) and Honghu Lake (S_L) in an ecologically fragile region in central China, were evaluated to reveal their phosphorus-adsorbing/desorbing properties and storage capacities. A nonlinear regression method was used to fit the pseudo-second-order kinetic and the modified crossover-type Langmuir isotherm models to the experimental data. It is shown that the adsorption of phosphorus onto the studied sediments followed the pseudo-second-order kinetic expression. The modified crossover-type Langmuir isotherm model was found to be a suitable method for describing adsorption/desorption processes in the experimental sediments. The maximum adsorption capacities (Q_m), partitioning coefficients (K_p), native adsorbed exchangeable phosphorus (NAP), and equilibrium phosphorus concentration (EPC_0) were subsequently obtained for the experimental sediments. The effects of sediment concentration and pH were also investigated by batch experiments and Fourier transformation infrared and scanning electron microscopy analyses. The adsorption/desorption characteristics of different phosphate species on the sediments from reservoir and lake buffer zones were identified.

Introduction

Increased eutrophication of freshwater often leads to a decrease in biodiversity, simplification of biotic community structure, instability of aquatic ecosystems, and increased turbidity of water (Qin et al. 2013). Excessive concentration of phosphorus, which has been identified as a key growth-limiting nutrient for algae, is the most common cause of eutrophication in freshwater reservoirs and lakes (Schindler 1977; Organization for Economic Cooperation and Development OECD 1982). Orthophosphate, which includes three ionized species of phosphoric acid ($H_2PO_4^{1-}$, HPO_4^{2-}, and PO_4^{3-}), is the only form of phosphorus that autotrophs can assimilate (Correll 1998). Phosphates in polluted surface runoff originate from several anthropogenic and natural sources, including: urban drainage, rural runoff, and drainage from natural phosphatic terrains (Kaufman 1975).

Riparian buffer zones adjacent to reservoirs or lakes act as natural filters, protecting aquatic ecosystems from polluted surface runoff. Healthy reservoir or lake buffer zones provide critical functions

L. Zhang (✉) · Y. Du · C. Du · M. Xu
Key Laboratory of Environment and Disaster Monitoring and Evaluation of Hubei, Institute of Geodesy and Geophysics, Chinese Academy of Sciences, Wuhan 430077, China
e-mail: lzhang@whigg.ac.cn

H. A. Loáiciga
Department of Geography, University of California, Santa Barbara, CA 93106, USA

for the improvement of surface water quality and storage of nutrients (Theriot et al. 2013). High capacity for phosphorus adsorption and retention by sediments from riparian areas can play a critical role in buffering some chemical and ecological changes and benefit aquatic environments (Wang and Li 2010). In contrast, native adsorbed exchangeable phosphorus (NAP) might be released from sediments under various environmental conditions, in which case these sediments become a source of phosphorus (Pan et al. 2002; Zhou et al. 2005).

Studies about phosphorus adsorption in natural sediments have been reported by several researchers over the past decades. Nevertheless, researching the adsorption/desorption characteristics of phosphorus in sediments of buffer zones remains a priority in ecologically fragile regions. China is a country with a large number of lakes and reservoirs, mostly distributed along the eastern coast and in the middle and lower Yangtze River basin. Most of the freshwater located in these regions suffers from water pollution caused by climatic variation and human activities (Le et al. 2010; Qin et al. 2013). Danjiangkou Reservoir is a water source for the Middle Route of China's South-to-North Water Transfer Project. This project will transfer 13 km^3 of water every year beginning in 2014. This diversion of water could profoundly change the aquatic environments of many impacted regions (Zhang 2009). including those of Danjiangkou Reservoir and Honghu Lake, selected for study in this work. Honghu Lake, located on the north bank of the middle reaches of the Yangtze River and near the Three Gorges Dam Project, contains the largest natural wetland in the Jianghan Plain in central China. During the past decades, the water quality of Honghu Lake has worsened gradually (Li et al. 2009).

Sediments from riparian buffer zones of Danjiangkou Reservoir and Honghu Lake were evaluated to (1) investigate their phosphorus adsorption/desorption characteristics, (2) assess their phosphorus storage capacities, and (3) reveal the effects of sediment concentration and their background pH on the aqueous system. The results from this type of research are significant for developing potential approaches, such as artificial modification of sediment chemistry, for riparian buffer zone management, restoration, and conservation.

Methods and materials

Sampling site description

Samples were collected from the riparian buffer zones of Danjiangkou Reservoir (S_R, sampling position: longitude 111° 28′ E and latitude 32° 35′ N) and Honghu Lake (S_L, sampling position: longitude 113° 25′ E and latitude 29° 48′ N), in central China. The samples were taken at locations about 2–3 m landward from the water bodies, at sites that were significantly affected by surrounding water and terrestrial ecosystems. The water surface area of Danjiangkou Reservoir will reach approximately 1022 km^2 after the South-to-North Water Transfer Project is completed. Honghu Lake has an area of approximately 344 km^2. These two study areas have subtropical monsoonal climates. The average annual precipitation at Danjiangkou Reservoir is approximately 900 mm, and the mean annual air temperature is about 15 °C. The average annual air temperature and annual precipitation of Honghu Lake area are approximately 18 °C and 1368 mm, respectively.

Analysis of freshwater buffer sediments

Surface sediments (0~20 cm deep) were collected from the buffer zones of Honghu Lake and Danjiangkou Reservoir, respectively. Several replicate samples were retrieved randomly at each site. Thereafter, they were prescreened to remove large gravel particles and woody fragments, finely ground and sieved to particle size <0.15 mm, and oven-dried at 170 °C for 2 h before experiments. A N_2 gas Brunauer–Emmett–Teller (BET) analysis was carried out to determine the sediments' surface area and adsorption average pore width by using a Micromeritics Chemisorption ASAP 2020. An X-ray fluorescence (XRF) spectrometer Bruker AXS S4 Pioneer was used for the composition analysis. Fourier transformation infrared (FT-IR) spectra were recorded at room temperature using a Nicolet 5700 FT-IR spectrometer. The FT-IR spectra were recorded in the 400 to 4000 cm^{-1} range and measured with a 4 cm^{-1} resolution. Scanning electron microscopy (SEM) measurement was carried out using a FEI Quanta 200 apparatus.

Experimental procedure for the study of adsorption kinetics

Two 5-L beakers were prepared by mixing 40 g of dried sediments and 1 L of liquid solution with the initial phosphorus concentration equal to 10 mg/L; 0.02 mol/L KCl was added as electrolyte to each solution. The kinetic experiments were conducted at 25 °C and at a constant agitation speed of 170 rpm; 5 mL of slurry was pipetted out at different times. The samples were centrifuged immediately for 1 min at 10,000 rpm at 25 °C and then filtered to completely separate the liquid and solid phases. The phosphorus solution was analyzed for the remaining phosphorus concentration according to the ammonium molybdate spectrophotometric method using a spectrophotometer.

Experimental procedure for the study of the adsorption/desorption isotherm

A synthetic phosphorus solution comprising distilled water and potassium dihydrogen phosphate was used. A stock solution of 500 mg/L was prepared by dissolving a weighed amount of phosphorus in 1000 mL of distilled water. The solution was prepared by diluting the stock solution with distilled water when necessary. Each experiment consisted of a series of initial phosphorus concentrations equal to 0, 0.2, 0.4, 1.0, 2.0, 3.0, 4.0, and 5.0 mg/L; 0.02 mol/L KCl was added as electrolyte to each solution. A weighed amount of the sediment samples was added to the solution. The conical flasks were then shaken at a constant speed of 170 rpm in a shaking water bath. The samples were centrifuged for 5 min at 8000 rpm with a HITACHI CR22GII High-Speed Refrigerated Centrifuge after shaking the flasks for 3 h, which was a sufficiently long reaction time for the uptake of phosphorus from aqueous solution. Subsequently, the samples were filtered to completely separate the liquid and solid phases. The phosphorus solution was analyzed for the remaining phosphorus concentration with a spectrophotometer. Batch experiments were run at 25 °C and at four initial sediment concentrations (C_S) ($C_S = 6$ g/L, for example, means 6 g of sediment per 1 L of phosphorus solution) equal to 6, 10, 20, and 40 g/L, respectively.

The effect of pH on the adsorption/desorption of phosphorus

Identical experimental procedures were conducted for sediment samples collected in the riparian buffer zones of Danjiangkou Reservoir and Honghu Lake. A series of batch experiments was run with different initial pH values and at constant temperature (25 °C). The initial pH values were adjusted with either 0.01, 0.1, or 1.0 M HCl or NaOH solution. Each experiment was run with the initial phosphorus concentration equal to 5.0 mg/L; 0.02 mol/L KCl was added as electrolyte to each solution. A weighed amount (1.0 g) of the sediment samples was added to the solution. The shaking, separation, and analysis procedures were the same as those of the method described in the section dealing with the adsorption/desorption isotherm.

Phosphorus adsorption/desorption capacity

The phosphorus adsorption/desorption capacity ($P_{A/D}$) was calculated with the following formula:

$$P_{A/D} = \left(P_{init} - P_{equil}\right) V / w \qquad (1)$$

in which $P_{A/D}$ is expressed in milligrams of phosphorus per gram of (dry) sediment, P_{init} = initial phosphorus concentration, P_{equil} = phosphorus concentration at equilibrium, V = volume of the phosphorus solution, and w = dry mass of sediments.

Results and discussion

Properties of sediments

Two kinds of sediments, namely buffer sediments from Danjiangkou Reservoir (S_R) and from Honghu Lake (S_L), were characterized using BET surface area and XRF spectrometric analyses. The surface area, adsorption average pore width, and elemental composition of the sediments are listed in Table 1. The adsorption rate of phosphorus is affected by the physical and chemical properties of the sediment, such as its metal oxide (Fe and Al) content and porosity. Generally, fine-textured sediments offer more active adsorption sites in the sediments, and the metal oxides are the predominant absorbents (Syers et al. 1973; Brinkman 1993).

Table 1 demonstrates similar characteristics for the two types of sediments (S_R and S_L), except that the

Table 1 Main chemical characteristics of experimental sediments

Chemical parameters	S_R (Danjiangkou Reservoir)	S_L (Honghu Lake)
BET surface area (m²/g)	11.66	11.28
Average pore width (nm)	6.12	10.16
Main elemental composition (% by weight)		
O	46.78	47.53
Si	27.12	27.98
Al	9.513	9.691
Fe	7.036	4.922
Ca	3.878	3.701
Na	1.960	0.632
Mg	1.927	1.583
K	1.050	2.649
Ti	0.300	0.600
C	0.113	0.381

Table 2 Pseudo-second-order kinetic parameters of phosphorus adsorption onto experimental sediments. The initial phosphorus concentration in solution was 10 mg/L

Parameters	S_R (Danjiangkou Reservoir)	S_L (Honghu Lake)
q_e (mg/g)	0.123	0.180
k (g/(mg min))	6.123	5.917
h (mg/(g min))	0.092	0.192
r^2	0.9907	0.9931

average pore width of S_L was about 39.8 % larger than that of S_R.

Adsorption kinetics

The kinetic characteristics of phosphorus adsorption in the two sediments (S_R and S_L) were analyzed using a pseudo-second-order kinetic model, which is expressed by Eqs. (2) and (3) (Ho and McKay 2000; Ho 2006; Ho and Ofomaja 2006):

$$\frac{dq_t}{dt} = k(q_e - q_t)^2 \qquad (2)$$

where k is the rate constant of adsorption (g/(mg min)), q_e is the amount of phosphorus adsorbed at equilibrium (mg/g), and q_t is the amount of phosphorus adsorbed at time t (mg/g). For initial conditions $q_t = 0$ at $t = 0$, the integrated nonlinear form of Eq. (2) is

$$q_t = \frac{q_e^2 kt}{1 + q_e kt} \qquad (3)$$

taking the derivative dq_t/dt in Eq. (3) and letting $t \to 0$ yield the initial adsorption rate h (mg/(g min)):

$$h = kq_e^2 \qquad (4)$$

Table 2 displays the experimentally derived pseudo-second-order kinetic parameters (q_e, k, h) of

phosphorus adsorption onto the S_R and S_L sediments corresponding to an initial phosphorus concentration equal to 10 mg/L.

The experimental phosphorus adsorption data were fitted with the pseudo-second-order model using nonlinear regression and are depicted in Fig. 1. The initial phosphorus concentration in solution used to develop the data shown in Fig. 1 was 10 mg/L. The uptake of phosphorus after 60 min approaches constant asymptotic values. The high value of the coefficients of determination for the two adsorbents ($r^2 > 0.99$) (see Table 2) indicates that the adsorption of phosphorus onto the tested sediments from riparian buffer zones is appropriately described by the pseudo-second-order kinetic model. Figure 1 shows a rapidly increasing adsorption in the first 10 min for the S_R and S_L sediments. However, the initial adsorption rate (h) of S_L sediments (0.192 mg/(g min)) was more than twice the rate for the S_R sediments (0.092 mg/(g min)).

The equilibrium isotherm

The Langmuir equilibrium isotherm has been widely used to describe the adsorption behavior of phosphorus from liquid solutions. The theoretical Langmuir isotherm is as follows (Langmuir 1918):

$$(C_{add} - C_e)V/w = \frac{Q_m C_e}{K_L + C_e} \qquad (5)$$

where C_{add} is the initial concentration of newly added phosphorus in solution of adsorption trials (mg/L), C_e is the equilibrium liquid-phase concentration (mg/L), V is the solution volume (L), w is the

Fig. 1 Phosphorus adsorption (q_t) onto S_R and S_L sediments as function of time (t) using the nonlinear pseudo-second-order kinetic model. The initial phosphorus concentration in solution was 10 mg/L
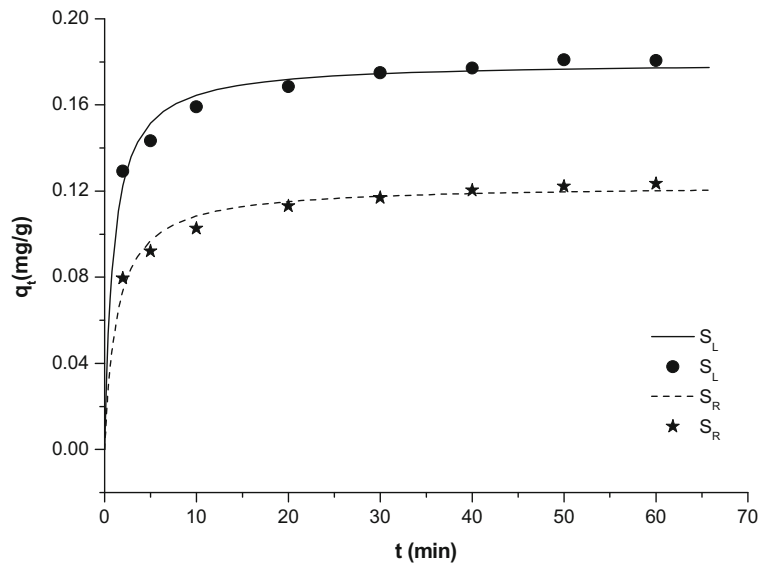
dry mass of sediment in the sorption trials (g), Q_m is the maximum adsorption capacity (mg/g), and K_L is the adsorption equilibrium constant (mg/L). Taking natively adsorbed exchangeable phosphorus (NAP, mg/g) into account, Eq. (5) becomes (Zhou et al. 2005)

$$\text{NAP} + \frac{(C_{add} - C_e)V}{w} = \frac{Q_m C_e}{K_L + C_e} \quad (6)$$

In the case of $C_{add} = 0$, Eq. (6) becomes

$$\text{NAP} = \frac{Q_m C_e^0}{K_L + C_e^0} + C_e^0 \frac{V}{w} \quad (7)$$

where C_e^0 is the equilibrium liquid-phase concentration of phosphorus (mg/L) when $C_{add} = 0$, which is equal to the solution concentration of phosphorus achieved at desorption equilibrium in freshwater. When NAP in Eq. (6) is replaced by Eq. (7), the modified equation is as follows:

$$\frac{(C_{add} - C_e)V}{w} = \frac{Q_m C_e}{K_L + C_e} - \left(\frac{Q_m C_e^0}{K_L + C_e^0} + \frac{C_e^0 V}{w} \right) \quad (8)$$

In terms of equilibrium phosphorus concentration (EPC$_0$), which refers to the liquid phase when $C_e = C_{add}$, then the expression for EPC$_0$ according to Eq. (8) is given by

$$\text{EPC}_0 = C_e = C_{add} = \frac{K_L Q_m C_e^0 / (K_L + C_e^0) + K_L C_e^0 V / w}{K_L Q_m / (K_L + C_e^0) - C_e^0 V / w} \quad (9)$$

The partitioning coefficient (K_p) is calculated with the following formula:

$$K_p = \frac{\text{NAP}}{\text{EPC}_0} \quad (10)$$

Table 3 displays the derived isotherm parameters of phosphorus adsorption (Q_m, K_L, K_p, NAP, EPC$_0$) onto S_R (Danjiangkou Reservoir) and S_L (Honghu Lake) sediments.

Nonlinear regression was used to fit the experimental data using Eq. (8) expressing the modified crossover-type Langmuir isotherms corresponding to four initial sediment concentrations (C_S) equal to 6, 10, 20, and 40 g/L. The results are shown in Fig. 2. The graphs in Fig. 2 show that the adsorption/desorption densities increase with increasing sediment concentration for a given initial phosphorus concentration in solution. The high r^2 values for S_R (>0.92) and S_L (>0.96) (see Table 3) indicate that the phosphorus adsorption/desorption processes in the S_R and S_L sediments are appropriately described by a modified crossover-type Langmuir equilibrium isotherm. The modified Langmuir isotherm approximated well the phosphorus adsorption on four types of sediments from

Table 3 Isotherm parameters of phosphorus adsorption onto experimental sediments

Sediment adsorbents	Sediment concentration (C_S) (g/L)	Fitting results			Calculated parameters		
		Q_m (mg/g)	K_L (mg/L)	r^2	NAP (mg/g)	EPC_0 (mg/L)	K_p (L/g)
S_R (Danjiangkou Reservoir)	6	0.139	1.389	0.9243	0.0012	0.0119	0.0989
	10	0.136	1.024	0.9670	0.0042	0.0324	0.1284
	20	0.111	0.696	0.9825	0.0037	0.0241	0.1545
	40	0.112	0.752	0.9831	0.0008	0.0052	0.1477
S_L (Honghu Lake)	6	0.230	1.441	0.9833	0.0146	0.0976	0.1493
	10	0.219	0.849	0.9865	0.0245	0.1071	0.2289
	20	0.199	0.609	0.9961	0.0160	0.0535	0.2999
	40	0.196	0.425	0.9620	0.0227	0.0558	0.4074

Fig. 2 The nonlinear modified crossover-type Langmuir isotherms corresponding to four initial sediment concentrations C_S equal to 6, 10, 20, and 40 g/L for S_R (**a**) and S_L (**b**) sediments as function of the initial phosphorus concentration in solution (mg/L)
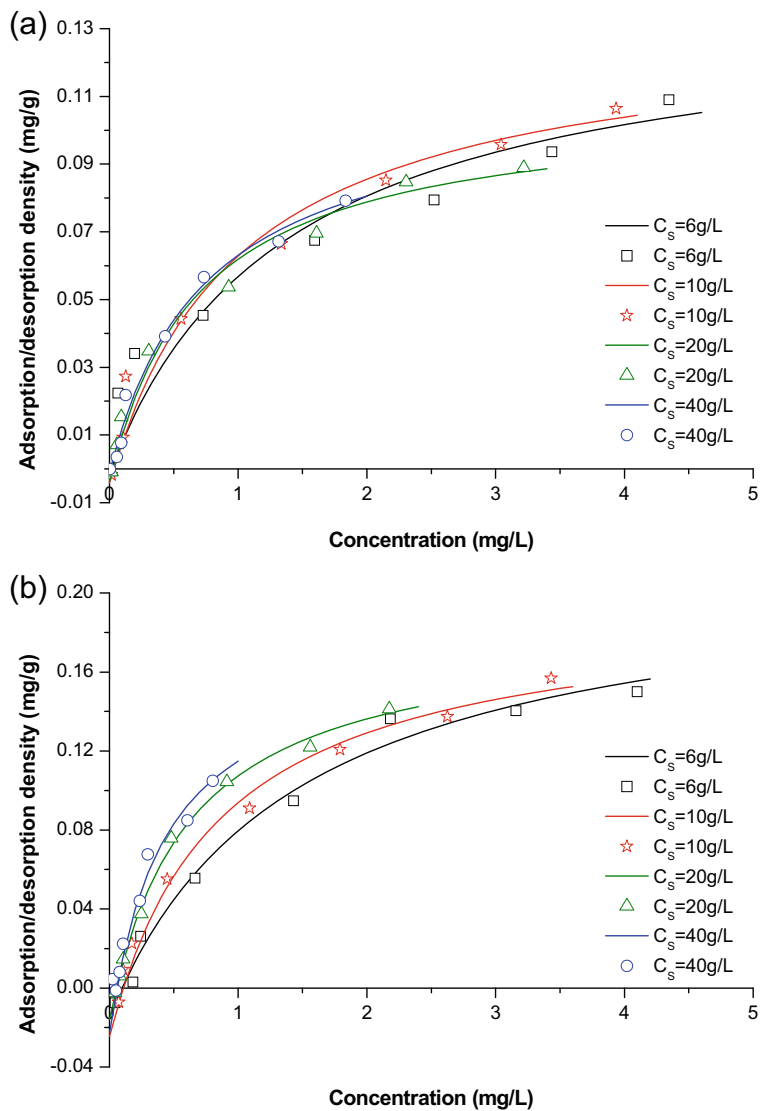
Dianchi Lake (in China), also, and the NAP, EPC$_0$, and Q_m were obtained subsequently (Huang et al. 2015).

The effect of sediment concentration on adsorption/desorption

As the initial sediment concentrations (C_S) increased from 6 to 40 g/L, the Q_m decreased from about 0.14 to 0.11 mg/g and from 0.23 to 0.20 mg/g for sediments S_R and S_L, respectively (see Table 3). Seven sediments from Danjiangkou Reservoir were used by Tang et al. (2014) to test the difference in phosphorus adsorption onto sediments. Their results indicated that the various compositions of the sediments caused differences in phosphorus adsorption capacities, and the Q_m, obtained with the Langmuir equation, ranged from 0.07 to 0.58 mg/g (Tang et al. 2014). Their calculated Q_m range was in agreement with our findings. But the Q_m of Dianchi Lake's sediments ranged from 0.54 to 41.47 mg/g, which is larger than those at Danjiangkou Reservoir and Honghu Lake (Chen et al. 2015). The partitioning coefficient (K_p) reflects the relative affinities of the solid and liquid phases for phosphorus. A large value of K_p indicates an enhanced affinity of phosphorus adsorption and retention on the solid phase (Zhou et al. 2005). It is seen in Table 3 that the K_p values increase from about 0.01 to 0.15 L/g and from 0.15 to 0.41 L/g for S_R and S_L, respectively, when the sediment concentration is raised from 6 to 40 g/L. The larger mean K_p value for S_L (0.2714 L/g) than for S_R (0.1324 L/g) demonstrates a larger phosphorus adsorption and retention capacity onto buffer sediments of Honghu Lake than that of Danjiangkou Reservoir sediments.

NAP refers to the phosphorus that is natively adsorbed onto sediments. Riparian buffer zones have the ability to retain nutrients, their sediments often contain NAP, and the isotherms with low initial phosphorus concentrations often cross over the liquid concentration axis (see Fig. 3) (Pan et al. 2002; Hoffmann et al. 2009). The average NAP of sediments S_R (0.0025 mg/g) is less than that of sediments S_L (0.0195 mg/g). This result is attributed to the surface water quality of the sediments at the sampling sites. The water qualities of the reservoir and lake significantly affect the NAP due to fluctuations in water level. Being a water source area of the Middle Route of China's South-to-North Water Transfer Project, Danjiangkou Reservoir's water quality meets the class II national water quality standard, which is a

very satisfactory standard. On the other hand, the water quality of Honghu Lake is not satisfactory because of the increased practice of aquaculture in the lake and uncontrolled nonpoint source pollution that reaches this lake (Zhang et al. 2012). It has been reported that high NAP values for the sediments from a eutrophic lake, Dianchi Lake, were in the range from 0.0297 to 0.0908 mg/g (Chen et al. 2015).

It is shown in Fig. 3 that the buffer sediments are neither sinks nor sources of phosphorus when the phosphorus concentration in solution is equal to EPC$_0$. When the phosphorus concentrations in solution are less than the value of EPC$_0$ (labelled as a desorption area in Fig. 3), the sediment serves as a source of phosphorus; when the phosphorus concentrations are greater than the value of EPC$_0$ (labelled as an adsorption area in Fig. 3), the sediment serves as a pool of phosphorus (Pan et al. 2002; Zhou et al. 2005). The mean EPC$_0$s for sediments S_R and S_L are 0.0184 and 0.0785 mg/L, respectively. These EPC$_0$ results indicate that the riparian buffer zone sediment of Honghu Lake was a plentiful source of phosphorus compared to that of the Danjiangkou Reservoir, when suffering from low phosphorus concentration runoffs. The NAP, EPC$_0$, and K_p for the buffer sediments vary with properties of the liquid solution, such as C_S and pH conditions.

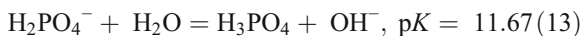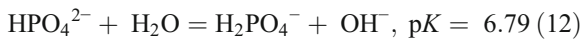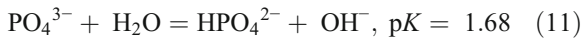## The effect of pH on adsorption/desorption

Different phosphorus solutions with several levels of initial pH (1.85 to 10.46) were prepared to assess the influence of pH on phosphorus adsorption/desorption. The low pH values (such as 1.85) seldom appear in the field. However, low pH values were also used in this experiment for specific purposes, such as observing sediment modification in the laboratory. Figure 4 shows that phosphorus adsorption/desorption by sediments is profoundly affected by pH. At a pH of 1.85, the Danjiangkou sediments S_R (desorption density 0.0170 mg/g) are a source of phosphorus, while the Honghu Lake sediments S_L (adsorption density 0.0806 mg/g) are a sink of phosphorus. The adsorption densities of S_R and S_L increase to 0.0952 and 0.1429 mg/g, respectively, when the pH equals 3.68 (pH$_a$). The variations of the adsorption densities of S_R and S_L become relatively stable when the pH increases to 8.85 (pH$_b$). Thereafter, the adsorption densities decrease with the increasing pH. The highest phosphorus adsorption densities of sediments S_R (initial pH = 8.85)

Fig. 3 The nonlinear modified crossover-type Langmuir isotherms corresponding to the initial sediment concentration C_S equal to 20 g/L for S_L (example only)
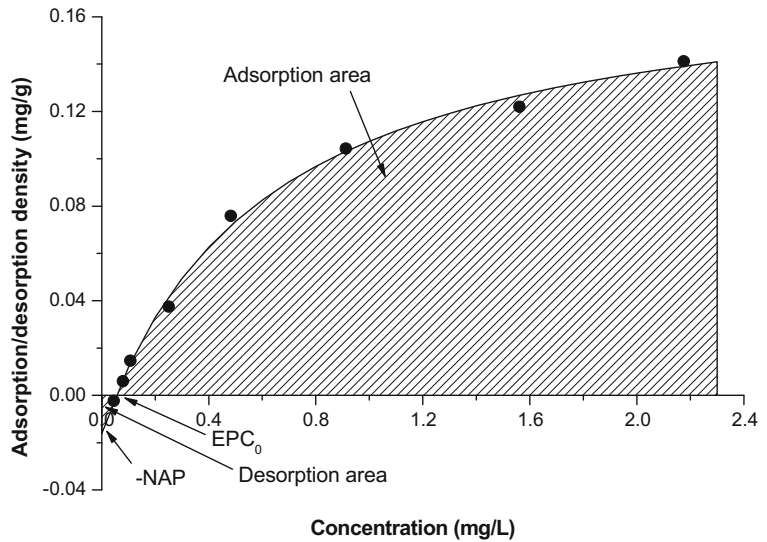
and S_L (initial pH = 3.68) are 0.0959 and 0.1429 mg/g, respectively.

KH$_2$PO$_4$ was used as the phosphate source in the experimental aqueous system. The speciation of phosphate might be present in various forms described by the following reactions with their corresponding pK at 25 °C (Clifford 1961; Karageorgiou et al. 2007; Oladoja et al. 2012):

$$PO_4^{3-} + H_2O = HPO_4^{2-} + OH^-, \ pK = 1.68 \quad (11)$$

$$HPO_4^{2-} + H_2O = H_2PO_4^- + OH^-, \ pK = 6.79 \quad (12)$$

$$H_2PO_4^- + H_2O = H_3PO_4 + OH^-, \ pK = 11.67 \quad (13)$$

From the phosphate distribution curves in Fig. 4, it is clear that H$_3$PO$_4$ is the main species in the aqueous system when the initial pH equals 1.85 (Hem 1985). The concentration of H$_2$PO$_4^-$ becomes significant when the initial pH of the solution equals pH$_a$. The H$_2$PO$_4^-$ and HPO$_4^{2-}$ species are present in the region between pH$_a$ and pH$_b$. This indicates that H$_2$PO$_4^-$ and HPO$_4^{2-}$ are the preferential sorption species of phosphorus onto the experimental sediments. In the region between pH$_a$ and pH$_b$, the sediment surface could compete strongly with H$^+$ to trap phosphate, and the phosphate had more ability than OH$^-$ to adsorb onto sediments.

The FT-IR results for sediments S_R and S_L before and after the adsorption experiments with different pH

Fig. 4 The influence of pH on the adsorption/desorption capacities of phosphorus onto S_R and S_L (*left vertical axis*) and distribution ratios of dissolved phosphate species activity as a function of pH (*right vertical axis*)
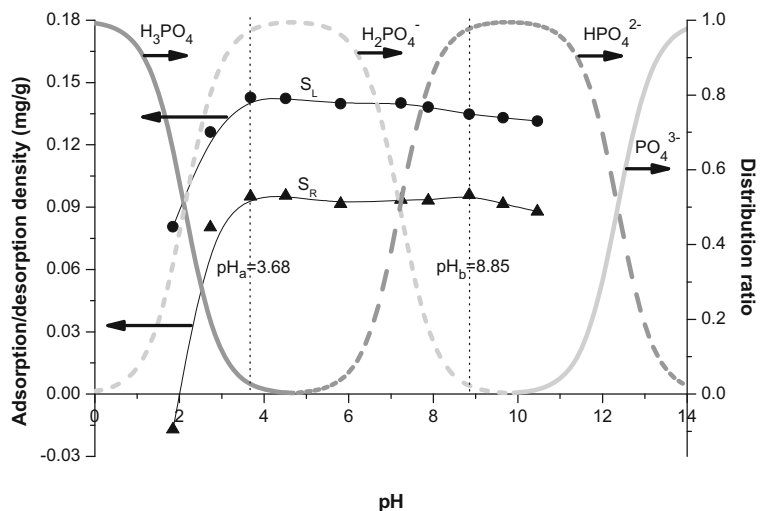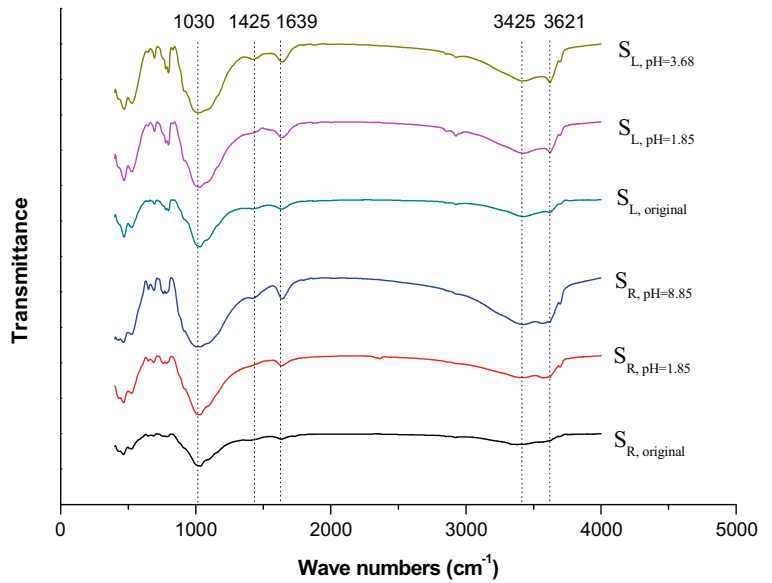
Fig. 5 Fourier transformation infrared (FT-IR) spectra of sediments

conditions are shown in Fig. 5. The Si–O–Si and Si–O–Moct (Moct = Fe, Al, and Mg) bending vibration bands appear within the 400 to 700 cm^{-1} region. The wave numbers near 1030 cm^{-1} are assigned to Si–O stretching vibrations of the tetrahedral sheets (Madejova et al. 2009). The wave numbers in the range 3425 to 3621 cm^{-1} are assigned as OH stretching vibrations, and the absorption band at 1639 cm^{-1} denotes the O–
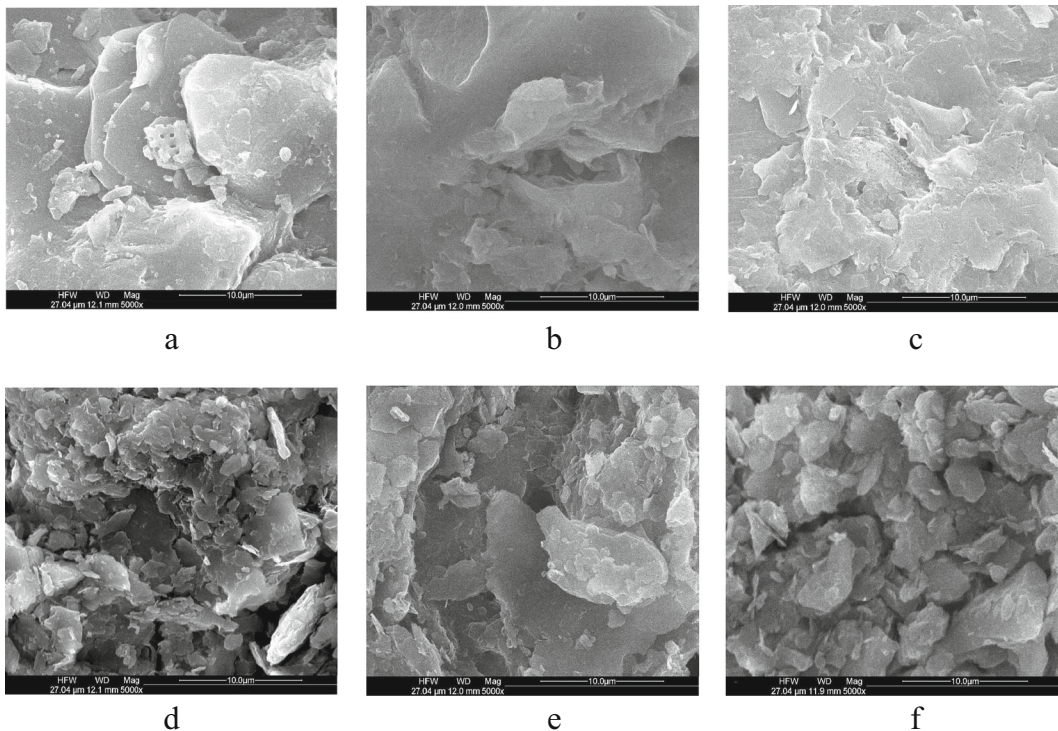

Fig. 6 Scanning electronic microscopy (SEM) for S$_R$ original samples (**a**) and samples treated by solutions with initial pH = 1.85 (**b**) and pH = 8.85 (**c**), and S$_L$ original samples (**d**) and samples treated by solutions with initial pH = 1.85 (**e**) and pH = 3.68 (**f**)

H water-bending mode (Chuang et al. 2008). By comparing the spectra before and after the adsorption experiments, there are no significant differences between the spectra in those regions between the original sediments and those with phosphorus at pH equal to 8.85 for S_R and pH equal to 3.68 for S_L. This finding proves that those microstructures mentioned above are not directly involved in the adsorption/desorption reactions.

It is seen in Fig. 5 that the absorption peaks near 1425 cm^{-1}, which is characteristic of calcium carbonate, are clearly reduced after treatment of the solution with initial pH of 1.85 (Du et al. 2008). The adsorption bands near the 3696 cm^{-1} region are assigned to OH stretching in kaolinite. This reduction after the adsorption reactions is caused by the replacement of the OH stretching by phosphate during the adsorption processes.

The phosphorus adsorption/desorption mechanism of the investigated water–sediment systems is supported by the visualization of electron scanning microscopy (SEM) images of the sediments (shown in Fig. 6). Panels a and d of Fig. 6 show the surface images of the original S_R and S_L sediments, respectively. The sediments' surfaces became smoother after the reactions with phosphorus solutions of initial pH = 1.85 according to Fig. 6b, e. This might be the reason causing the lower adsorption capacity for sediments S_L and the higher phosphorus desorption for sediments S_R. Figure 6b clearly shows that there are small particles attached to larger particles on the surface of sediments S_R, which are a source of phosphorus (desorption density = 0.0170 mg/g with pH = 1.85). The sediments S_R and S_L show their highest phosphorus adsorption capacities (adsorption density 0.0959 and 0.1429 mg/g, respectively) when the initial solution pH = 8.85 (see Fig. 6e) and pH = 3.68 (Fig. 6f), respectively. There are small particles that appear after the experiments, and the spacing between minerals is reduced because most of the gaps are occupied by the generated small complex compounds after the adsorption experiments (Xue et al. 2009). Our results indicate that the adsorbing properties of the studied sediments from reservoir and lake buffer zones are related to the phosphate exchange and precipitation reactions that occur in them.

Conclusions

The nonlinear pseudo-second-order model appropriately quantified the sorption process and indicated a rapider

initial adsorption rate of S_L than of S_R. The nonlinear modified crossover-type Langmuir isotherms demonstrated a larger phosphorus adsorption and retention capacity onto buffer sediments of Honghu Lake than of Danjiangkou Reservoir sediments. The riparian buffer zone sediment of Honghu Lake is a plentiful source of phosphorus compared to that of the Danjiangkou Reservoir, which exhibits runoff with low phosphorus concentration. The maximum adsorption capacities decreased when the sediment concentration was raised from 6 to 40 g/L. Sediments showed higher adsorbing capacities when the initial pH ranged between 3.68 and 8.85.

References

Brinkman, A. G. (1993). A double-layer model for ion adsorption onto metal oxides, applied to experimental data and to natural sediments of Lake Veluwe, The Netherlands. *Hydrobiologia, 253*, 31–45.

Chen, C. Y., Deng, W. M., Xu, X. M., He, J., Wang, S. R., Jiao, L. X., & Zhang, Y. (2015). Phosphorus adsorption and release characteristics of surface sediments in Dianchi Lake, China. *Environmental Earth Science, 74*, 3689–3700.

Chuang, Y. H., Tzou, Y. M., Wang, M. K., Liu, C. H., & Chiang, P. N. (2008). Removal of 2-chlorophenol from aqueous solution by Mg/Al layered double hydroxide (LDH) and modified LDH. *Industrial and Engineering Chemistry Research, 47*, 3813–3819.

Clifford, A. F. (1961). *Inorganic chemistry of quantitative analysis*. New Jersey: Prentice Hall.

Correll, D. L. (1998). The role of phosphorus in the eutrophication of receiving waters: a review. *Journal of Environmental Quality, 27*, 261–266.

Du, C., Linker, R., & Shaviv, A. (2008). Identification of agricultural Mediterranean soils using mid-infrared photoacoustic spectroscopy. *Geoderma, 143*, 85–90.

Hem, J. D. (1985). *Study and interpretation of the chemical characteristics of natural water*. Alexandria, Virginia: US Geological Survey Water Supply Paper 2254.

Ho, Y. S. (2006). Review of second-order models for adsorption systems. *Journal of Hazardous Materials, 136*, 681–689.

Ho, Y. S., & McKay, G. (2000). The kinetics of sorption of divalent metal ions onto sphagnum moss peat. *Water Research, 34*, 735–742.

Ho, Y. S., & Ofomaja, A. E. (2006). Kinetic studies of copper ion adsorption on palm kernel fibre. *Journal of Hazardous Materials, 137*, 1796–1802.

Hoffmann, C. C., Kjaergaard, C., Uusi-Kamppa, J., Hansen, H. C. B., & Kronvang, B. (2009). Phosphorus retention in riparian buffers: review of their efficiency. *Journal of Environmental Quality, 38*, 1942–1955.

Huang, W., Lu, Y., Li, J., Zheng, Z., Zhang, J. B., & Jiang, X. (2015). Effect of ionic strength on phosphorus sorption in different sediments from a eutrophic plateau lake. *Royal Society of Chemistry Advances, 5*, 79607–79615.

Karageorgiou, K., Paschalis, M., & Anastassakis, G. N. (2007). Removal of phosphate species from solution by adsorption onto calcite used as natural adsorbent. *Journal of Hazardous Materials, 139*, 447–452.

Kaufman, M. I. (1975). Generalized distribution and concentration of orthophosphate in Florida streams. U.S. Geol. Surv. Map Series 33 (revised).

Langmuir, I. (1918). The adsorption of gases on plane surfaces of glass, mica, and platinum. *Journal of the American Chemical Society, 40*, 1361–1403.

Le, C., Zha, Y., Li, Y., Sun, D., Lu, H., & Yin, B. (2010). Eutrophication of lake waters in China: cost, causes, and control. *Environmental Management, 45*, 662–668.

Li, T., Cai, S. M., Yang, H. D., Wang, X. L., Wu, S. J., & Ren, X. Y. (2009). Fuzzy comprehensive-quantifying assessment in analysis of water quality: a case study in Lake Honghu, China. *Environmental Engineering Science, 26*, 451–458.

Madejova, J., Pentrak, M., Palkova, H., & Komadel, P. (2009). Near-infrared spectroscopy: a powerful tool in studies of acid-treated clay minerals. *Vibrational Spectroscopy, 49*, 211–218.

Oladoja, N. A., Ahmad, A. L., Adesina, O. A., & Adelagun, R. O. A. (2012). Low-cost biogenic waste for phosphate capture from aqueous system. *Chemical Engineering Journal, 209*, 170–179.

Organization for Economic Cooperation and Development (OECD). (1982). *Eutrophication of waters: monitoring, assessment and control*. Paris: OECD.

Pan, G., Krom, M. D., & Herut, B. (2002). Adsorption-desorption of phosphate on airborne dust and riverborne particulates in East Mediterranean seawater. *Environmental Science and Technology, 36*, 3519–3524.

Qin, B. Q., Gao, G., Zhu, G. W., Zhang, Y. L., Song, Y. Z., Tang, X. M., Xu, H., & Deng, H. (2013). Lake eutrophication and its ecosystem response. *Chinese Science Bulletin, 58*, 961–970.

Schindler, D. W. (1977). Evolution of phosphorus limitation in lakes. *Science, 195*, 260–262.

Syers, J. K., Harris, R. F., & Armstrong, D. E. (1973). Phosphate chemistry in lake sediments. *Journal of Environmental Quality, 2*, 1–14.

Tang, X. Q., Wu, M., Dai, X. C., & Chai, P. H. (2014). Phosphorus storage dynamics and adsorption characteristics for sediment from a drinking water source reservoir and its relation with sediment compositions. *Ecological Engineering, 64*, 276–284.

Theriot, J. M., Conkle, J. L., Pezeshki, S. R., DeLaune, R. D., & White, J. R. (2013). Will hydrologic restoration of Mississippi River riparian wetlands improve their critical biogeochemical functions? *Ecological Engineering, 60*, 192–198.

Wang, Q. R., & Li, Y. C. (2010). Phosphorus adsorption and desorption behavior on sediments of different origins. *Journal of Soils and Sediments, 10*, 1159–1173.

Xue, Y., Hou, H., & Zhu, S. (2009). Characteristics and mechanisms of phosphate adsorption onto basic oxygen furnace slag. *Journal of Hazardous Materials, 162*, 973–980.

Zhang, Q. F. (2009). The South-to-North Water Transfer Project of China: environmental implications and monitoring strategy. *Journal of the American Water Resources Association, 45*, 1238–1247.

Zhang, L., Du, Y., Wu, S. J., Yu, C., Feng, Q., Ban, X., Ren, X. Y., & Xue, H. P. (2012). Characteristics of nutrients in natural wetland in winter: a case study. *Environmental Monitoring and Assessment, 184*, 5487–5495.

Zhou, A. M., Tang, H. X., & Wang, D. S. (2005). Phosphorus adsorption on natural sediments: modeling and effects of pH and sediment composition. *Water Research, 39*, 1245–1254.